- PLAYING WITH THE LATTICE POTENTIAL

* Now that what know the basics of atoms in optical lattices, it's a good idea to discuss a bit about the possibilities offered in experiments for the manipulation of atoms in optical lattices.

· Interestingly the parameters of the problem may be changed (almost) at will!

- Tunnel rate (t) → as we will soon see it may be controlled by means of lattice modulations
- Interactions (U) → they may be modified using Feshbach resonances (I'll not discuss that)
- One may have other form of interactions → this we will see in more detail when we discuss polar gases.
- Lattice geometry → the lattice may have more involved geometries than simply square or cubic (e.g. triangular, honeycomb, etc) [We will come back to this later]
- Disorder → we may add disorder using speckle or another incommensurate lattice.
- Synthetic magnetism → even for neutral atoms! [I'll discuss this later]

And many of these things may be done in real time! This plays an important role in the next discussion.

* LATTICE SHAKING

* Interestingly, the sign of t and its absolute value may be modified by means of a <u>periodic modulation of the lattice Hamiltonian</u> [Eckardt et al., PRL 95, 260404 (2005)]. Let's have a brief look to the idea (we restrict to a 1D case).

* Let's consider a <u>periodically forced Bose-Hubbard Hamiltonian</u> described by the explicitely time-dependent form:

$$\hat{H}(t) = \hat{H}_0 + K\cos(\omega t)\sum_j j\,\hat{n}_j$$ where $\hat{H}_0$ is the Hubbard Hamiltonian

* The oscillating term can be realized experimentally by periodically shifting the position of a mirror employed to generate the standing laser wave forming the optical lattice, and transforming to the co-moving reference frame. [*Note: If we shake the lattice as $x(t) = \Delta x\cos\omega t$, in the lattice frame we obtain an inertial force: $F = -m\ddot{x} = m\omega^2\Delta x\cos\omega t$, and hence an oscillating on-site energy $V_j = -x_j \cdot F = [-\lambda\Delta x\, m\omega^2]\cos\omega t\, j = K\cos\omega t\, j$, as above.]

* Note that $\hat{H}(t) = \hat{H}(t+T)$ with $T = 2\pi/\omega$. The analysis of the problem is hence done better by means of <u>quantum Floquet theory</u>, which resembles Bloch theory of periodic potentials but now in time instead of space:

We write the solutions of the time-dependent many-body Schrödinger equation in the form:

$$|\psi_n(t)\rangle = |u_n(t)\rangle \exp\{-i\varepsilon_n t/\hbar\}$$ with $|u_n(t)\rangle = |u_n(t+T)\rangle$
$\Downarrow$
<u>Floquet states</u>.

* The Floquet states are obtained by solving the eigenvalue equation:

$$\left[\hat{H}(t) - i\hbar\partial_t\right]|u_n(t)\rangle = \varepsilon_n |u_n(t)\rangle$$

with ε_n the <u>quasi-energies</u> defined up to an integer multiple of $\hbar\omega$ (like quasimomenta in Bloch's theory)

* If $|u_n(t)\rangle$ solves the eigenvalue equation with eigenvalues ε_n, then $|u_n(t)\rangle e^{im\omega t}$ is a T-periodic eigensolution with energy $\varepsilon_n + m\hbar\omega$ $(m = 0, \pm 1, \pm 2, \dots)$. The quasienergy spectrum has hence a <u>Brillouin-zone-like</u> structure (the width of the Brillouin zone is $\hbar\omega$).

* We introduce the Floquet basis:

$$|\{n_j\},m\rangle = |\{n_j\}\rangle \exp\left[-i\frac{K}{\hbar\omega}\sin\omega t \sum_j j\, n_j + i m\omega t\right]$$

Fock state with n_j particles at site j

We'll see right now why we add this here!

. The eigenvalue problem refers to an extended Hilbert space of T-periodic functions, in which the time is regarded as a coordinate. We hence introduce the scalar product:

$$\langle\langle\cdot|\cdot\rangle\rangle = \frac{1}{T}\int_0^T dt\, \langle\cdot|\cdot\rangle$$ (i.e. usual scalar product combined with time-averaging within one period)

To solve the eigenvalue problem we compute the matrix elements of $\hat{H}(t) - i\hbar\partial_t$ in the Floquet basis $|\{n_j\},m\rangle$ with respect to this scalar product:

. Let $\hat{H}_0 = \hat{H}_{TUN} + \hat{H}_{INT}$ with $\hat{H}_{TUN} = -t\sum_{\langle ij\rangle} b_i^\dagger b_j$

Note that $-i\hbar\partial_t |\{n_j\},m\rangle = \left[-K\cos\omega t \sum_j n_j + i m\omega\right]|\{n_j\},m\rangle$.

This removes the periodic part of $\hat{H}(t)$ and hence:

$$\langle\langle\{n_j'\},m'|\hat{H} - i\hbar\partial_t|\{n_j\},m\rangle\rangle = \langle\langle\{n_j'\},m'|\hat{H}_{TUN} + \hat{H}_{INT} + i m\omega|\{n_j\},m\rangle$$

* Let's have a look to the hopping part:

$$\langle\langle\{n_j'\},m'|\hat{H}_{TUN}|\{n_j\},m\rangle\rangle = \frac{1}{T}\int_0^T dt\, \langle\{n_j'\}|\hat{H}_{TUN}|\{n_j\}\rangle e^{+i\frac{K}{\hbar\omega}\sin\omega t\sum_j j(n_j'-n_j)} e^{i(m-m')\omega t}$$

Since $\hat{H}_{TUN}$ just transfers one particle from a site to a neighbouring one then $\sum_j (n_j'-n_j)\, j = \pm 1 \equiv s$.

Then:

$$\langle\langle\{n_j'\},m'|\hat{H}_{TUN}|\{n_j\},m\rangle\rangle = \frac{1}{T}\int_0^T dt\, \langle\{n_j'\}|\hat{H}_{TUN}|\{n_j\}\rangle e^{i(m-m')\omega t} e^{i\frac{Ks}{\hbar\omega}\sin\omega t} \underset{\omega t=\theta}{=}$$

$$= \langle\{n_j'\}|\hat{H}_{TUN}|\{n_j\}\rangle \underbrace{\frac{1}{2\pi}\int_0^{2\pi} d\theta\, e^{i(m-m')\theta} e^{i\frac{Ks}{\hbar\omega}\sin\theta}}_{J_{m-m'}\left[\frac{Ks}{\hbar\omega}\right] = s^{m-m'} J_{m-m'}\left(\frac{K}{\hbar\omega}\right)}$$

Bessel function

* On the other hand

$$\langle\{n_j\},m'|H_{INT}+im\omega|\{n_j\},m\rangle = \delta_{m'm}\left[\langle\{n_j'\}|H_{INT}|\{n_j\}\rangle + m\hbar\omega\right]$$

Then:

$$\langle\langle\{n_j'\},m'|\hat{H}(t)-i\hbar\partial_t|\{n_j\},m\rangle\rangle = \delta_{m'm}\left[m\hbar\omega + \langle\{n_j'\}|J_0\left(\frac{K}{\hbar\omega}\right)H_{tun} + H_{INT}|\{n_j\}\rangle\right]$$

$$+(1-\delta_{m'm})\,S^{m'-m}\,J_{m'-m}\left(\frac{K}{\hbar\omega}\right)\langle\{n_j'\}|H_{tun}|\{n_j\}\rangle$$

* We get hence diagonal blocks (with $m'=m$) in which we recover the original Hamiltonian but now $t\to t\,J_0(K/\hbar\omega)$. Each block is separated from a neighboring one by an energy $\hbar\omega$.

The blocks are coupled by non-diagonal terms proportional to $J_{m'-m}\left(\frac{K}{\hbar\omega}\right)$. These couplings may be neglected if $\hbar\omega$ is much larger than any other energy scale $[\hbar\omega \gg t, U]$.

* If this is so we get hence something remarkable. As mentioned above we recover the original Hamiltonian but now

$$\boxed{t \longrightarrow t\,J_0\left(\frac{K}{\hbar\omega}\right)} \equiv J_{eff}$$

but recall that the Bessel function J_0 behaves as:

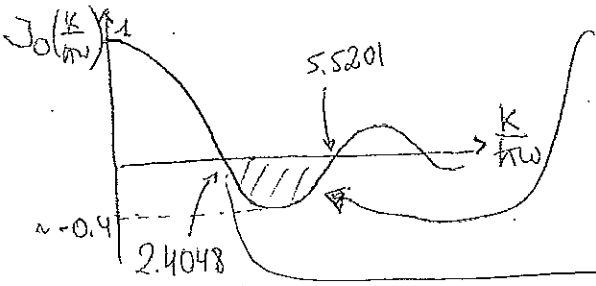

we may hence modify the sign of the hopping constant (!!)

We may switch-off the hopping as well!!

* Hence, hard core bosons (with the "shaking" trick) allow for the simulation of ferromagnetic and antiferromagnetic planar spins.

* This trick was first experimentally realized by the group of O. Morsch/E. Arimondo in Pisa [Lignier et al, PRL 99, 220403(2007)], and more recently in the group of K. Sengstock in Hamburg. [Struck et al., Science 333, 996 (2011)]

↳ see p. 57

* The first experiment that applied the idea of lattice shaking to atoms in optical lattice was performed in Pisa in the group of E. Arimondo in 2007. Let's briefly review this experiment.

After loading a BEC into a 1D optical lattice, they switched on a frequency modulation of one of the lattice beams (inducing lattice shaking). They then performed two different types of experiments:

(a) They switched off the trap along the direction of the lattice, leaving the radial confinement. The BEC expanded then freely along the lattice direction (via tunneling). The in-situ width was measured using absorption imaging. The growth of the condensate width (w_x) along the lattice is linear in time, and $d\sigma_x/dt$ is directly related to $|J_{eff}|$. They obtained in this way $|J_{eff}|$ which depend exactly as it should, i.e. as a Bessel function (see p. 58)

(b) The previous experiment was not sensitive to the sign of J_{eff}. In order to study that they performed time-of-flight measurements.

- If $J_{eff} > 0$ the band dispersion is like this 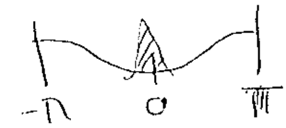

and hence we expect interference fringes at $0, \pm 2\hbar k, \pm 4\hbar k, \ldots$
- If $J_{eff} < 0$ $\longrightarrow$ 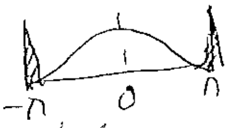

$\longrightarrow$ and hence we expect the fringes at $\pm \hbar k, \pm 3\hbar k, \ldots$

They observed this change in the interference fringes exactly at $K/\hbar\omega \simeq 2.4$ as one would expect from the Bessel function dependence (p. 58)

The study as well the phase coherence of the BEC (given by the fringe visibility); as expected when $J_{eff} \to 0$ the coherence is lost. (p. 58)

Lattice shaking [Lignier et al., PRL **99**, 220403 (2007)]

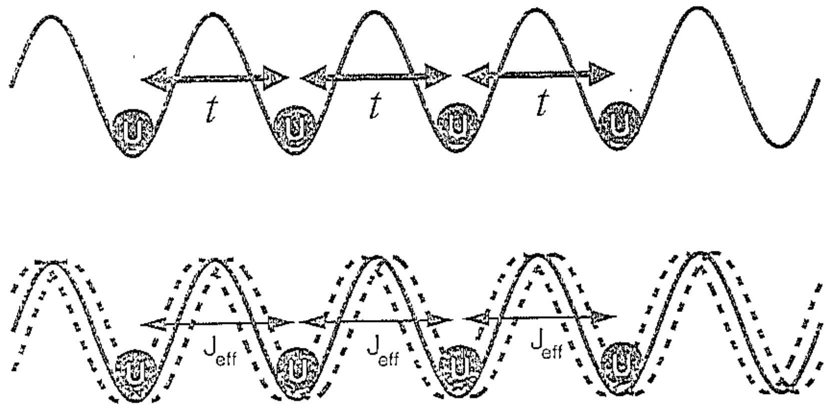

Obtained from the analysis of the expansion in the lattice when removing harmonic confinement.

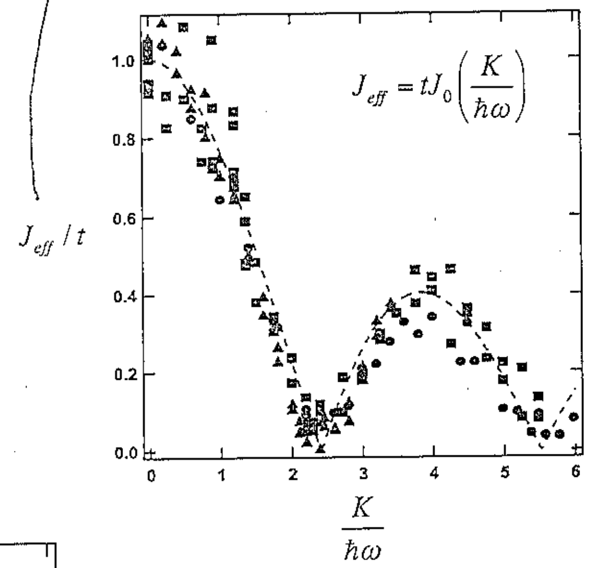

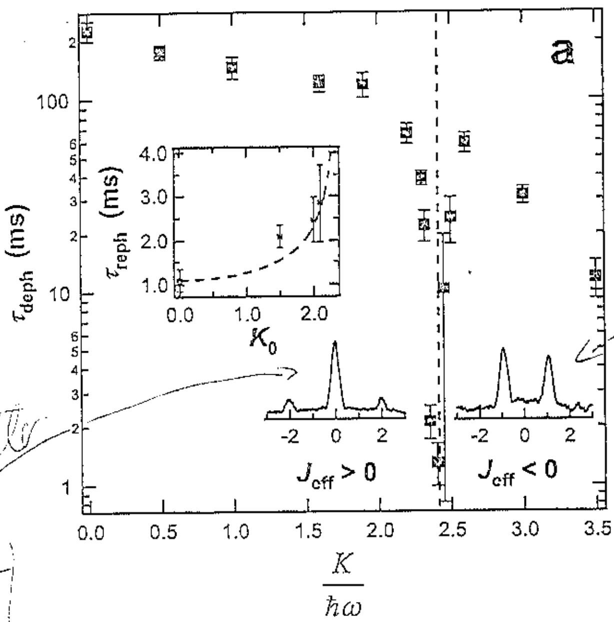

peak in the center

1BZ ⇒

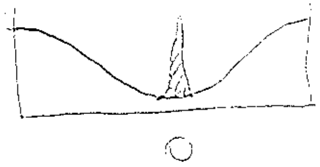

peak at π

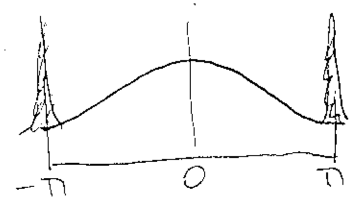

(due to the inversion $J \to -J$)

* Using lattice shaking one may modify significantly the lattice dispersion. We will discuss a couple of examples from the groups of C. Chin (Chicago) and K. Sengstock (Hamburg). Let's start with an experiment of 2013 at Chicago, in which lattice shaking was employed to induce effective "ferromagnetic" domains of cold atoms in an optical lattice.

* A BEC was loaded in a 1D lattice. They then employed lattice shaking at a frequency near the ground-band to first-excited-band transition.

As shown in the figure, one creates in this way a hybridized band structure. By adjusting the amplitude of the shaking one can tune the dispersion from one with a single minimum to one with 2 distinct minima (p. 60).

· As you can see from the figures of p. 60 when 2 minima develop all of the atoms are in one or in the other minimum. Since both minima are degenerated we have here an example of spontaneous symmetry breaking. This symmetry breaking results from the interactions. That's easy to see from a 2-mode model, with the 2 minima labelled as ↑ and ↓. For a uniform system, we get an effective Hamiltonian:

$$H = \overset{\text{energy of the minima}}{\varepsilon}(N_\uparrow + N_\downarrow) + \frac{g}{2}(N_\uparrow^2 + N_\downarrow^2) + 2g N_\uparrow N_\downarrow$$

↳ due to the Hartree and Fock interactions

Defining $J_z = \frac{1}{2}(N_\uparrow - N_\downarrow)$, $N = N_\uparrow + N_\downarrow$ $\rightarrow$ $H = \underbrace{\varepsilon N + \frac{3g}{4}N^2}_{\text{constant}} \underbrace{- g J_z^2}_{\text{favors "ferromagnetism"}}$ (i.e. it minimizes for $J_z = \pm N/2$)

· Interactions favor hence one or the other minimum.

Modifying the lattice dispersion [Parker et al., Nat. Phys. 9, 769 (2013)]

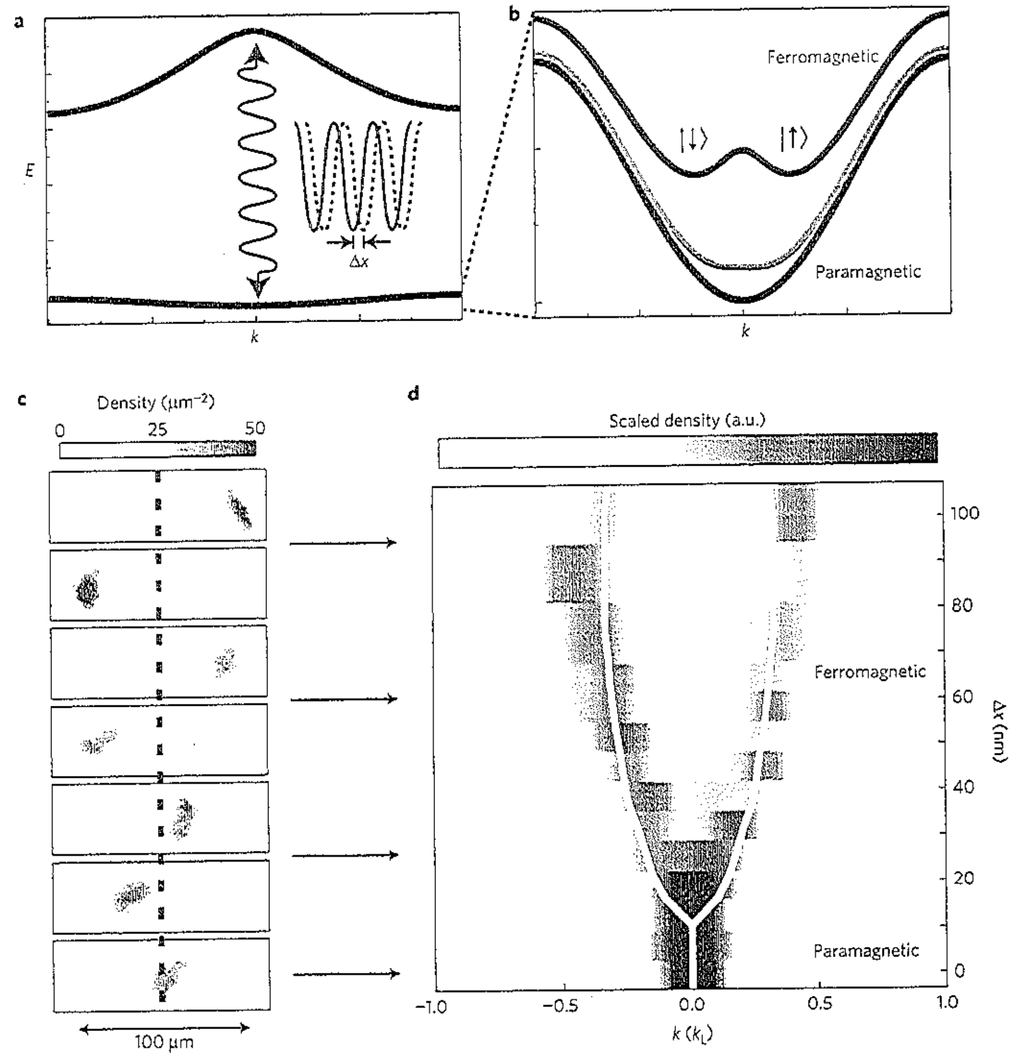

6a

Modifying the lattice dispersion [Parker et al., Nat. Phys. **9**, 769 (2013)]

Ramping-up the shaking leads to the formation of ferromagnetic domains (Kibble-Zurek mechanism)

The faster the ramp the more domains are formed

Slow ramp

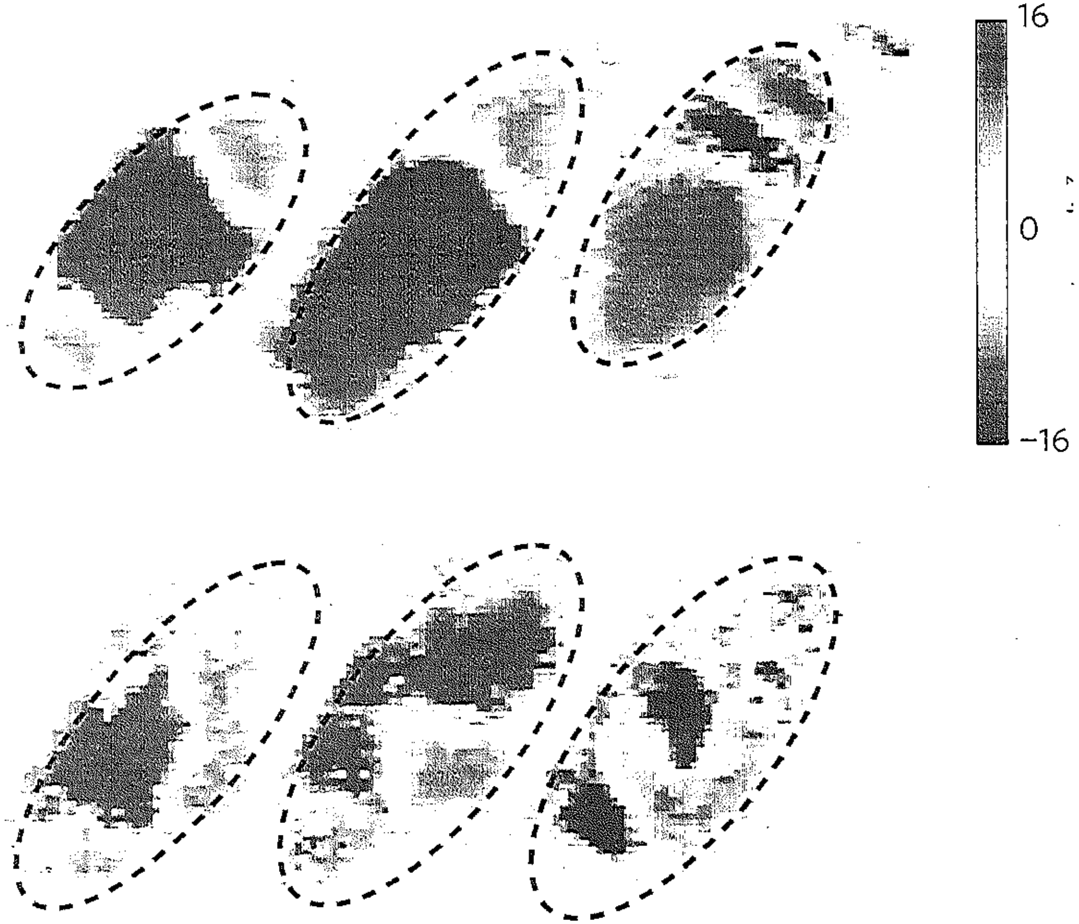

Fast ramp

TRIANGULAR LATTICES

- Up to now we have only considered a simple lattice geometry, namely a square (or cubic lattice). A square lattice is obtained by using 2 pairs of counterpropagating lasers.
- However, proper laser arrangements allow for more complicated (and potentially more interesting) lattice geometries.
- Let's consider for example the case of a triangular lattice, which may be created using 3 laser beams [Becker et al., NJP 12, 065025 (2010)]

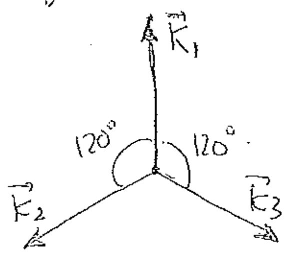

$$\left.\begin{aligned} &\bullet\ \vec{k}_1 = k(0,1) \\ &\bullet\ \vec{k}_2 = k\left(-\tfrac{\sqrt{3}}{2}, -\tfrac{1}{2}\right) \\ &\bullet\ \vec{k}_3 = k\left(\tfrac{\sqrt{3}}{2}, -\tfrac{1}{2}\right) \end{aligned}\right\}$$

- We add the field strengths of the individual beams coherently

$$\vec{E}(\vec{r},t) = \sum_{i=1}^{3} E_{0i}\,\vec{e}_i \cos[\vec{k}_i\cdot\vec{r} - \omega t + \phi_i]$$

← dephase

amplitude (we assume $E_{0i} = E_0$ for all beams)

polarization (we assume for all of them linear polarization along $z \to \vec{e}_i = \vec{e}_z$)

- The dipole potential created by this laser arrangement is proportional to the field intensity $|\vec{E}(\vec{r},t)|^2$

$$|\vec{E}(\vec{r},t)|^2 = \sum_{i,j} |E_0|^2 \Big\{ \cos(\vec{k}_i\cdot\vec{r}+\phi_i)\cos(\vec{k}_j\cdot\vec{r}+\phi_j)\cos^2\omega t + \sin(\vec{k}_i\cdot\vec{r}+\phi_i)\sin(\vec{k}_j\cdot\vec{r}+\phi_j)\sin^2\omega t + [\cos(\vec{k}_i\cdot\vec{r}+\phi_i)\sin(\vec{k}_j\cdot\vec{r}+\phi_j) + \sin(\vec{k}_i\cdot\vec{r}+\phi_i)\cos(\vec{k}_j\cdot\vec{r}+\phi_j)]\cos\omega t \sin\omega t \Big\}$$

Averaging over time

$$\overline{|\vec{E}(\vec{r})|^2} = \sum_{i,j} \frac{|E_0|^2}{2} \cos[(\vec{k}_i - \vec{k}_j)\cdot\vec{r} + \underbrace{(\phi_i - \phi_j)}]$$

The relative phases are stabilized (locked) in the experiment. We fix them here to zero.

· Let $\vec{b}_1 \equiv (\vec{k}_2 - \vec{k}_3) = k(-\sqrt{3}, 0)$

$\vec{b}_2 \equiv (\vec{k}_1 - \vec{k}_3) = \frac{\sqrt{3}}{2} k (1, \sqrt{3})$

Then the potential experienced by the atoms is (apart from constants) of the form:

$$V(\vec{r}) = V_0 \left[\cos(\vec{b}_1 \cdot \vec{r}) + \cos(\vec{b}_2 \cdot \vec{r}) + \cos[(\vec{b}_1 - \vec{b}_2) \cdot \vec{r}] \right]$$

This is a periodic potential. The reciprocal lattice is given by the vectors $\vec{b}_1$ and $\vec{b}_2$. We may then easily evaluate the primitive direct lattice vectors, which fulfill $\vec{a}_i \cdot \vec{b}_j = 2\pi \delta_{ij}$. A simple calculation gives:

$$\left.\begin{aligned} \vec{a}_1 &= \frac{4\pi}{3k}\left(-\frac{\sqrt{3}}{2}, \frac{1}{2}\right) \\ \vec{a}_2 &= \frac{4\pi}{3k}(0, 1) \end{aligned}\right\}$$

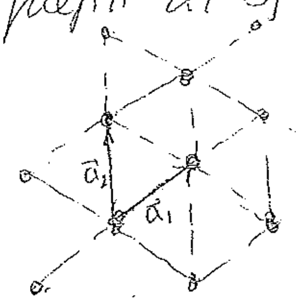

$\Rightarrow$ We obtain hence a triangular lattice! (see p. 64).

* Interestingly one may modify the hoppings in the lattice using the shaking technique discussed in p. 64, such that we get different hopping rates (and eventually with different sign) along $\vec{a}_1$ or $\vec{a}_2$ [Eckhardt et al., EPL 89, 10010 (2010)].

One moves the lattice along an elliptical orbit

$$\vec{X}(t) = \Delta X_c \cos\omega t \, \vec{e}_c + \Delta X_s \sin\omega t \, \vec{e}_s$$

The resulting inertial force in the lattice frame is

$$\vec{F}(t) = -m\ddot{\vec{X}} = F_c \cos\omega t \, \vec{e}_c + F_s \sin\omega t \, \vec{e}_s \qquad \text{with} \quad F_{c,s} = m\omega^2 \Delta X_{c,s}$$

· The Hubbard Hamiltonian is then given by:

$$\hat{H}(t) = -\sum_{\langle ij \rangle} t \, \hat{b}_i^\dagger \hat{b}_j + \frac{U}{2} \sum_i \hat{n}_i (\hat{n}_i - 1) + \sum_i [v_i(t) - \mu] \hat{n}_i$$

where $v_i(t) = -\vec{F}(t) \cdot \vec{r}_i$

· Using a similar analysis as that of p. 64, this shaking may be translated into an effective hopping rate:

$$t_{ij}^{eff} = t \, J_0\left[\frac{K_{ij}}{\hbar\omega}\right] \qquad \text{with} \quad K_{ij} = \sqrt{(F_c \vec{e}_c \cdot \vec{r}_{ij})^2 + (F_s \vec{e}_s \cdot \vec{r}_{ij})^2}$$

$$\vec{r}_{ij} = \vec{r}_i - \vec{r}_j$$

Triangular lattice [Becker et al., New J. of Phys. **12**, 065025 (2010)]

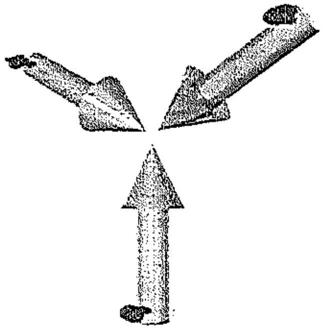

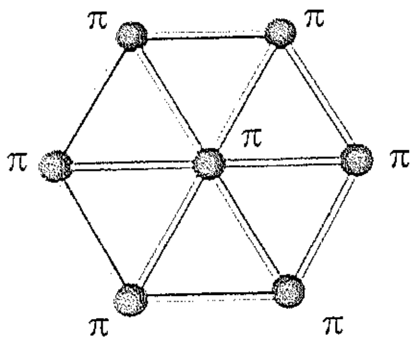

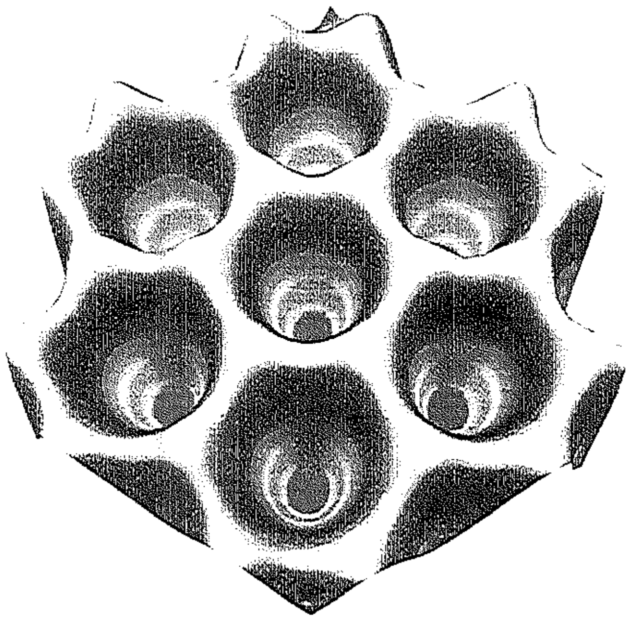

* Let $\vec{e}_c = \vec{e}_y$, $\vec{e}_s = \vec{e}_x$, we get then two different tunneling rates (see figure)

$\Delta x_{c,d} = d$ (lattice constant)

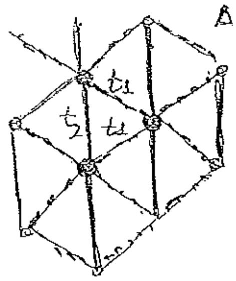

• $t_1 = t J_0\left(\frac{K_1}{\hbar\omega}\right)$ with $K_1 \equiv \frac{d}{2}\sqrt{F_c^2+3F_s^2}$

• $t_2 = t J_0\left(\frac{K_2}{\hbar\omega}\right)$ with $K_2 \equiv d\,|F_c|$

• We may hence obtain any value of the ratio $\frac{t_1}{t_2}$.

This has been recently employed for studying interesting phases of condensates in triangular lattices in the group of Klaus Sengstock in Hamburg [Struck et al., Science 333, 996 (2011)].

In those experiments the local phase of the condensate at a given lattice site is mapped onto a classical spin vector $\nearrow\Phi$...

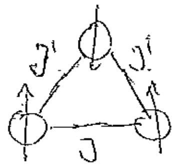

• The coupling $J \equiv t_2$ and $J' \equiv t_1$ may be tuned ferro- or antiferromagnetically, determining the resulting spin configuration (i.e. the condensate phase distribution).

• For example if both couplings are ferro you get

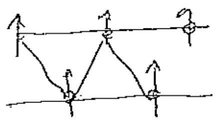

If J' is AF but J is F

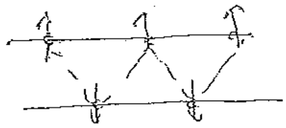

• The funniest situation occur when J is AF, since this leads to frustration i.e. it isn't immediately obvious where the spins should point. Let's see this

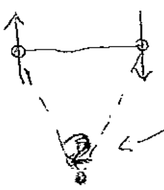

It's clear that we can't place here ↑ or ↓ without breaking the F or AF character of at least one bond.

• What one gets is actually an spiral. For J' AF:

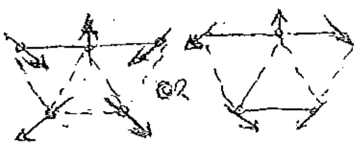

and for J' Ferro:

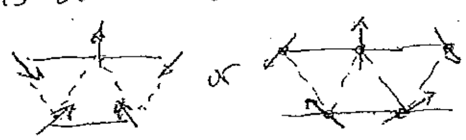

• Frustration is actually one of the most fascinating topics of quantum magnetism, which may be studied with ultra-cold lattice gases.

Frustrated classical antiferromagnetism [Struck et al., Science **333**, 996 (2011)]

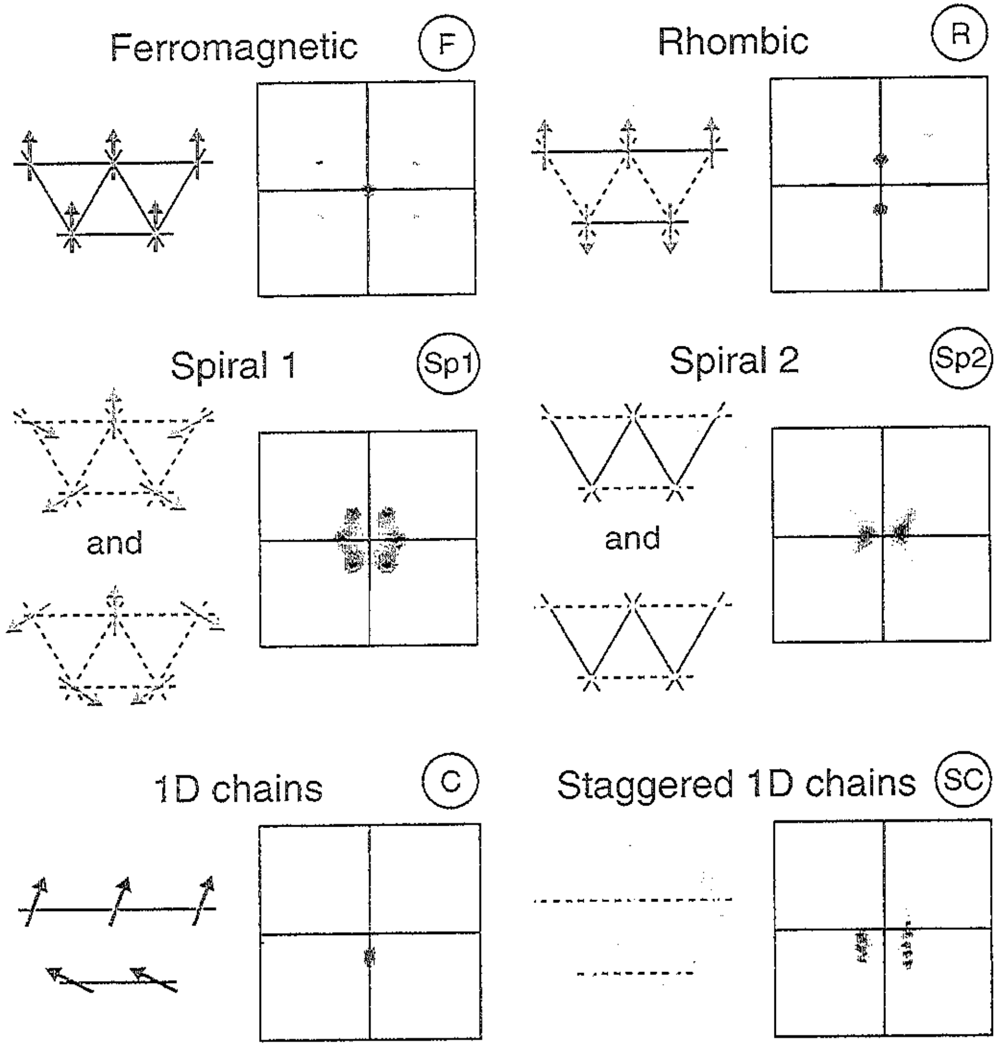

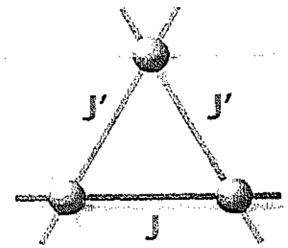

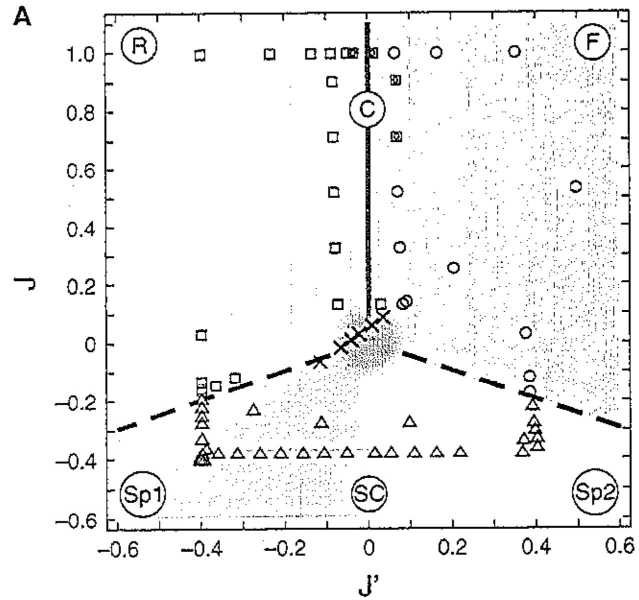

Frustrated classical antiferromagnetism [Struck et al., Science **333**, 996 (2011)]

One minimum (rombic phase) becomes two minima (spiral phase). Note what happens at the transition. The minimum becomes quartic along one direction. This indicates a poor superfluidity along that direction, and hence blurred interference fringes

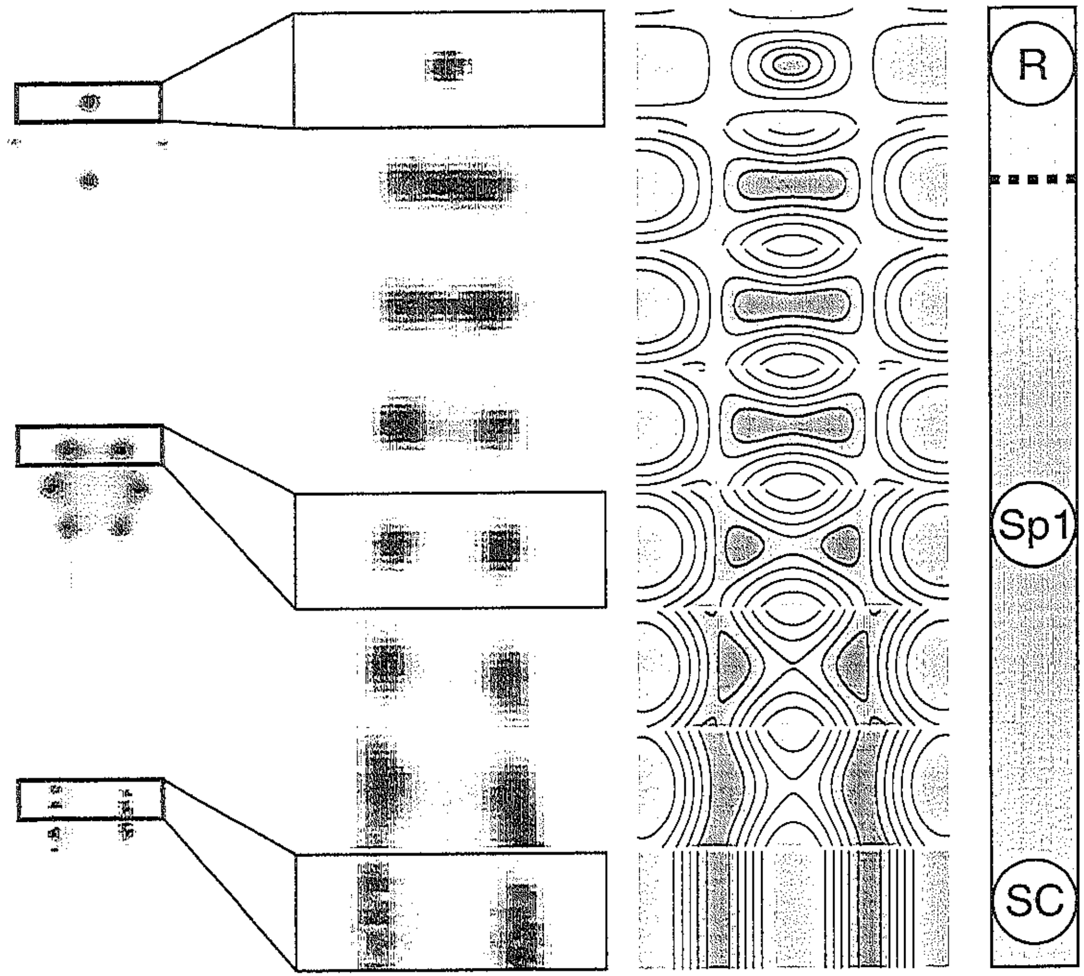

Experimental data

Dispersion relation

* In order to see even more clearly the effects of frustration in this type of problems we are going to consider at this point a related scenario, namely <u>a zig-zag lattice</u>

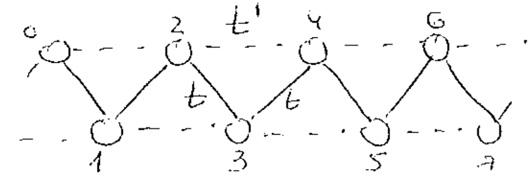

* let's forget for the moment interactions. The Bose-Hubbard model is of the form:

$$H = -t\sum_j (b^+_{j+1} b_j + \mathrm{H.c.}) - t'\sum_j (b^+_{j+2} b_j + \mathrm{H.c.})$$

. Let's introduce the Fourier transform:

$$b_j = \frac{1}{\sqrt{L}}\sum_K b_K e^{iKj} \quad \text{with } L \text{ the number of sites}$$

Then:
$$H = -t\,\frac{1}{L}\sum_{K,K'} b^+_K b_{K'} \sum_j e^{-iK(j+1)} e^{iK'j} + \mathrm{H.c.}$$

$$\frac{1}{L}\sum_j e^{ikj} = \delta_{k,0}$$

$$- t'\,\frac{1}{L}\sum_{k,k'} b^+_k b_{k'} \sum_j e^{-ik(j+2)} e^{ik'j} + \mathrm{H.c.} =$$

$$= -t\sum_K (e^{-ik} + e^{ik})\, b^+_k b_K - t'\sum_k (e^{-2ik} + e^{2ik})\, b^+_k b_k$$

$$= -2\sum_K (t\cos K + t'\cos 2K)\, b^+_k b_k$$

the band dispersion is hence $\varepsilon(k) = -2[t\cos k + t'\cos 2k]$. However if

If $t, t' > 0$ the energy minimum is at $k = 0$. However if $t' < 0$ (and we can change the sign of t' using shaking)

then:

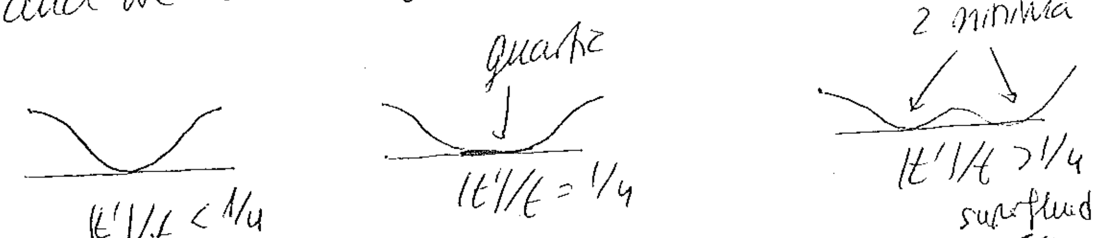

. For a filling factor $\langle n\rangle = 1$ one will have a superfluid for $|t'|/t < 1/4$, but for $|t'|/t > 1/4$ interactions prefer one or the other minimum (so-called chiral superfluid phase, which for zig-zag quantum ladders corresponds roughly with the spiral phases observed in Hamburg).

. For $|t'|/t = 1/4$ a quartic dispersion occurs, and as a result the Mott-insulator phase goes for $|t'|/t = 1/4$ all the way down to $U \to 0$.

This shows how bizarre can be the physics for "flat" bands!

Zig-zag lattices [Greschner et al., PRA 87, 033609 (2013)]

As a result of the strong frustration at $|t'|/t=1/4$, a MI may occur all the way to zero interactions!

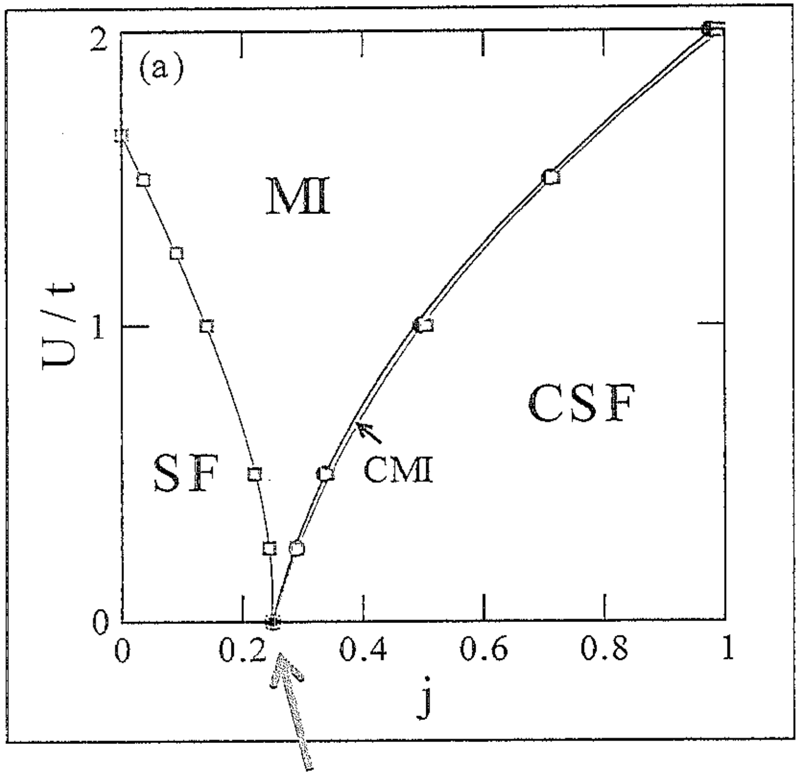

Lifshitz-point (j=1/4)

TWO-DIMENSIONAL OPTICAL LATTICE OF VARIABLE GEOMETRY

The lattice geometry may be modified in various ways. Let's comment at this point briefly on an experiment of T. Esslinger's group in 2012 [Tarruell et al., Nature 302, 483 (2012)]. In that experiment they developed a 2D optical lattice of adjustable geometry. The lattice is formed by 3 retro-reflected laser beams (of wavelength λ)

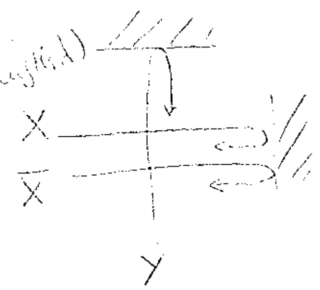

* The interference of the X and Y beams results in a checkerboard lattice of spacing $\frac{\lambda}{\sqrt{2}}$
* A third beam $\bar{X}$ collinear with X but detuned by a frequency δ creates an additional standing wave with spacing $\lambda/2$

· The overall potential is then:

$$V(x,y) = -V_{\bar{X}} \cos^2(kx + \theta/2) - V_X \cos^2(kx) - V_Y \cos^2(ky) - 2\alpha\sqrt{V_X V_Y}\cos(kx)\cos(ky)\cos\varphi$$

visibility of the interference pattern

They fix $\theta = \pi$, $\varphi = 0$ and by varying $V_{\bar{X}}$, V_X and V_Y they can reach different geometries (see p. 71).

* In that experiment they focus in particular on the creation of a honeycomb lattice

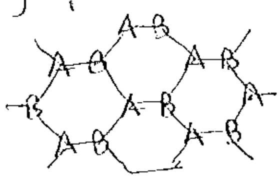

This is a lattice which may be split into 2 sublattices

· As a result 2 lowest sub-bands are formed (well separated from higher bands). The 2 bands have a conical intersection at 2 quasimomentum points in the Brillouin zone (see p. 71). These are the so-called Dirac points. This points act as topological defects in the band structure. I will come back in a later stage to this issue.

Honeycomb lattices (and more...) [Tarruell et al., Nature **483**, 302 (2012)]

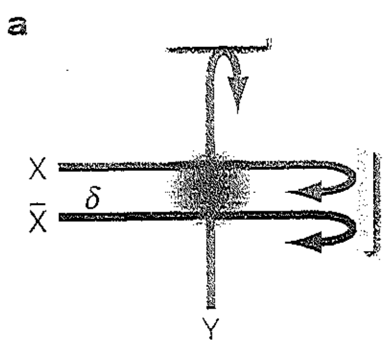

$$V(x,y) = -V_{\bar{X}}\cos^2(kx+\theta/2) - V_X\cos^2(kx) - V_Y\cos^2(ky) - 2\alpha\sqrt{V_X V_Y}\cos(kx)\cos(ky)\cos(\varphi)$$

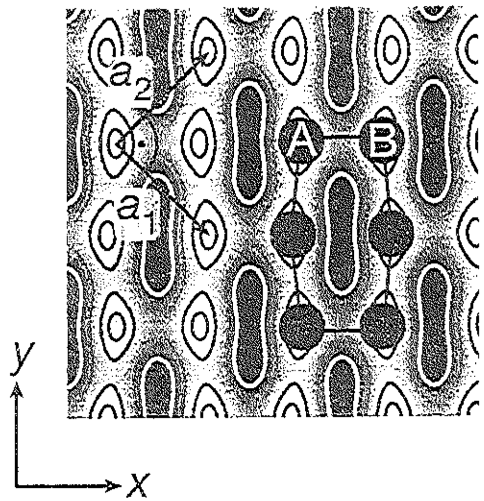

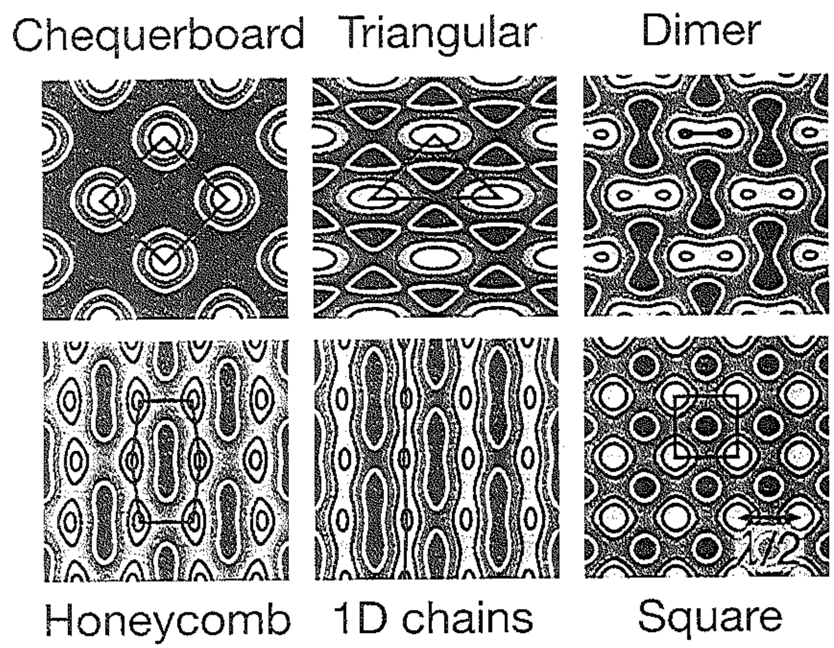

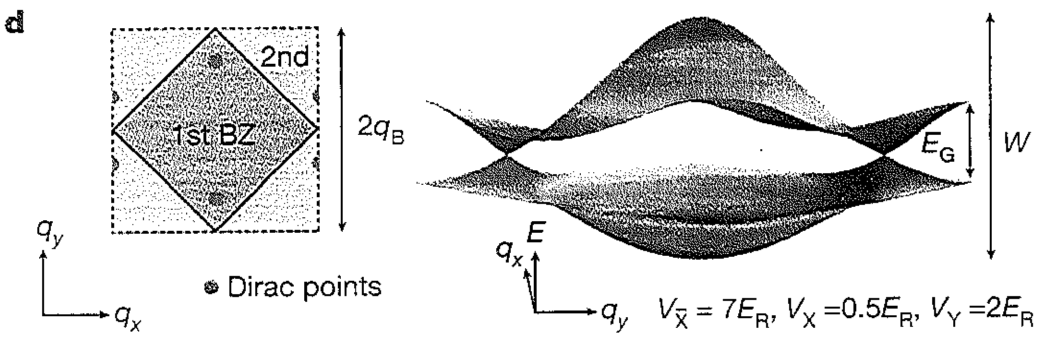

* KAGOMÉ LATTICES

* As mentioned above, 3 plane waves of equal intensity I, equal frequency (ω) and equal $|\vec{k}|$ (and polarization perpendicular to the xy plane) lying in the xy-plane and intersecting at equal angles, produce a triangular lattice of intensity minima. If we employ a <u>blue-detuned</u> lattice (with respect to the atomic transition) then the atoms experience as mentioned above, a triangular lattice of potential minima. [Note: In blue-detuned lattices, intensity minima are potential minima]

* Note from fig (64) that the intensity maxima (of intensity $\frac{9}{2}I$) form a honey-comb lattice. The maxima are separated by a triangular lattice of saddle-points with intensity $4I$ (indicated by o)

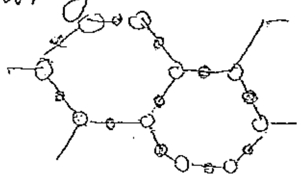

. If the lasers are <u>red-detuned</u>, then the potential <u>minima are at the density maxima! → one has a</u> <u>honey-comb lattice</u> with the same token!

*

* A combination of a blue-detuned and a red-detuned lattice has been recently employed at the group of D. Stamper-Kurn [Jo et al., PRL 108, 045305 (2012)] to create a so-called <u>Kagomé lattice</u>

They use two lattices (both triangular, created with 3 lasers, but one with $|\vec{k}|$ and the other $|\vec{k}|/2$)

- One with lattice spacing $a/2$ and blue detuned (SW-lattice)
- One with lattice spacing a and red detuned (LW-lattice)

* A unit cell of the LW-lattice has 4 sites of SW-lattice (see figure in p. 43) A, B, C, D. We may align the lattices such that D coincides with an LW-potential maximum. This lowers the energies of sites A, B, C, giving a barrier $\Delta V = V_D - V_{A,B,C} = \frac{8}{9}\underbrace{V_{LW}}_{}$ → depth of the LW lattice

When ΔV increases atoms are excluded from the D sites. The

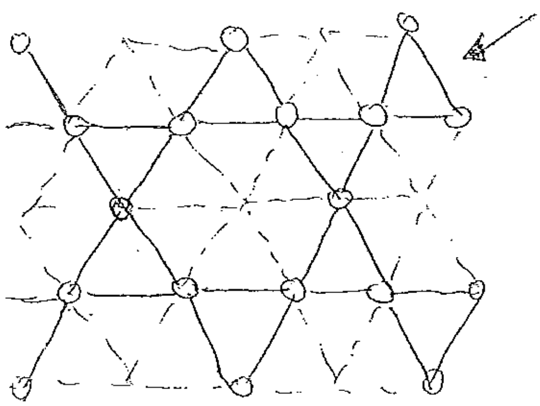

remaining sites form a Kagomé lattice which persists for $V_{LW} > 9 V_{SW}$ ↳ depth of the SW lattice.

- Kagomé lattices possess interesting properties (including a geometrically induced flat band)

Its quantum magnetic properties are actually not fully understood (<u>highly frustrated system</u>)

Kagome lattices [Jo et al., PRL **108**, 045305 (2012)]

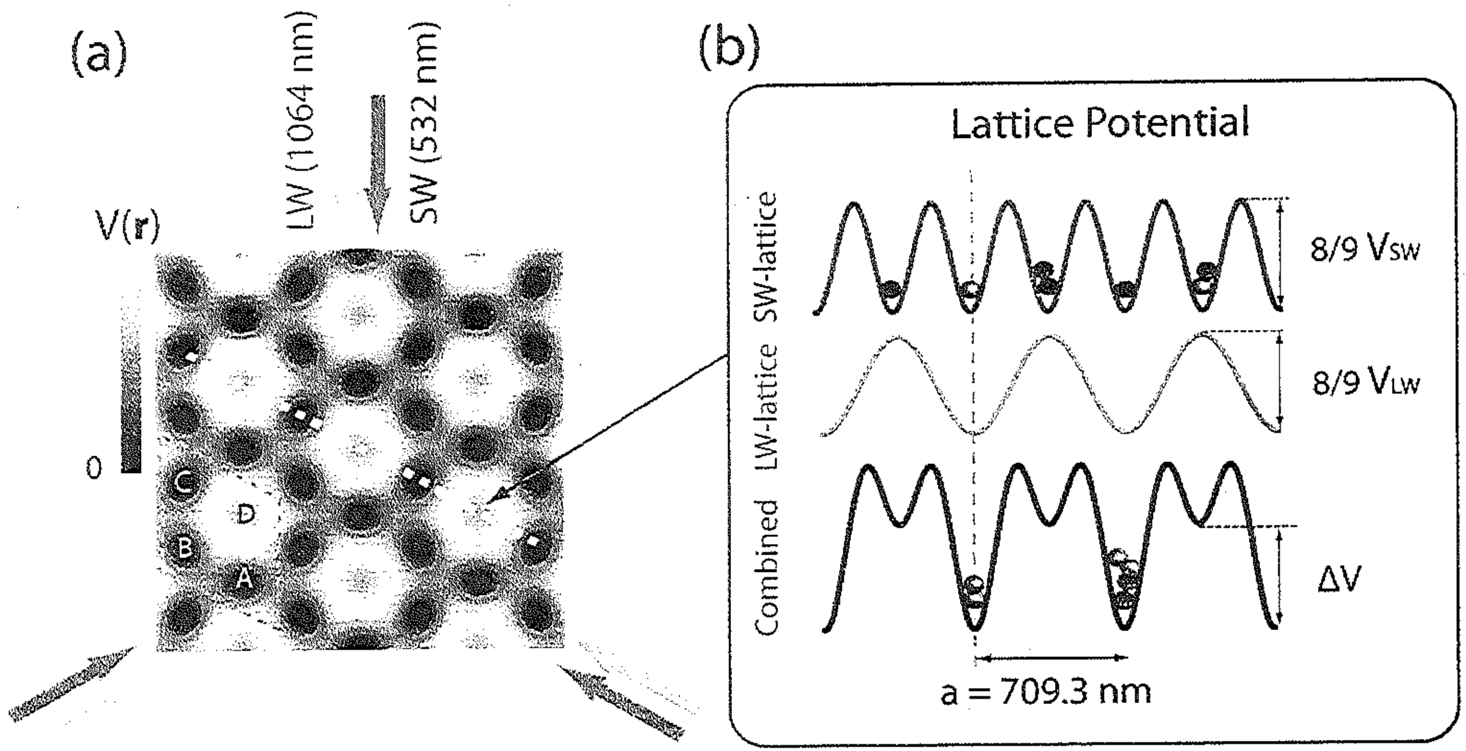

* P-BANDS : ORBITAL SUPERFLUIDITY

* Up to now we have considered that the atoms are always loaded in the lowest band of the lattice (this is the S-band).
* Interestingly one may populate as well higher bands controllably, opening quite fascinating possibilities. One may e.g. populate p-bands.

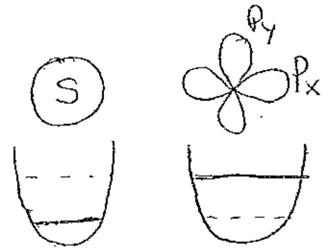

* The on-site wave functions look then like in the picture.
* This is quite interesting because it opens the possibility of playing with the orbital degree of freedom (i.e. p_x, p_y), whereas for an S-band this degree of freedom was "boring" (always S).

* Particularly interesting in this sense are recent experiments performed at Andreas Hemmerich's group in Hamburg [Wirth et al, Nat. Phys. 7, 147 (2010)].
* They use the laser arrangement depicted in p. 76. This allows them to create a square lattice composed of two classes of (tube-shaped) lattice sites (A and B). By playing with the relative phase θ between the plane waves that form the lattice (see p. 77) one can control the relative depth of sites A and B.
* This may be employed to transfer atoms into an upper band (p. 78). One starts with much deeper B sites (the atoms are in the B minima). One then makes the A sites deeper and then one populates a higher band (it's clear that the A sites are not any more in the ground state). One may then populate the P-band.
* After a short while the atoms condense in the P-band. Note that the P-band has in principle 2 degenerated points at its border (see the points in p. 77). One may control experimentally the relative depth of these minima of the P-band, making them equal (symmetric configuration) or unequal (asymmetric configuration).

* Page 78 shows results for an asymmetric case. After a short holding time 2 pronounced peaks are observed in the band mapping corresponding to a condensation in blue (or red) points in p. 77. Time-of-flight pictures (p. 78) show the appearance of Bragg peaks showing cross-dimensional coherence.

- The symmetric configuration looks however different (p. 77) since it shows four peaks. One has there a coherent admixture of both red and blue minima.

Interestingly repulsive interactions favour for a symmetric configuration $p_x \pm i p_y$ complex orbitals, corresponding to a local angular momentum $\pm \hbar$. To maximize intersite hopping, the local phases of adjacent orbitals match at their tunneling junction (see p. 79).

One gets then complex BEC wavefunctions [Cai and Wu, PRA 84, 033635 (2011)] of the form:

$$\psi(\vec{r}) = \left(\psi_{BLUE}(\vec{r}) + e^{\pm i\pi/2}\, \psi_{RED}(\vec{r}) \right)/\sqrt{2}$$

(This complex condensation has been termed orbital superfluidity in Wirth et al.)

* If one breaks the symmetry between the band minima, the energy difference may beat the repulsion energy, and eventually real BECs occur in which either blue or red minima are populated. The orbitals present in that case the striped form depicted in p. 79, and one recovers 2 maxima in the band mapping instead of 4. One gets here $p_x \pm p_y$ orbital at sites A (instead of $p_x \pm i p_y$).

- There's hence a competition between band anisotropy (which favors real BEC) and repulsion (which favors complex BEC). As a result there's a second-order phase transition between complex and real BEC for finite values of the asymmetry.

* The possibility of playing with the orbital degree of freedom opens exciting possibilities for strongly-correlated lattice gases as well, as e.g. the possibility of simulating spin-orbital models.

P-bands [Wirth et al., Nature Physics 7, 147 (2010)]

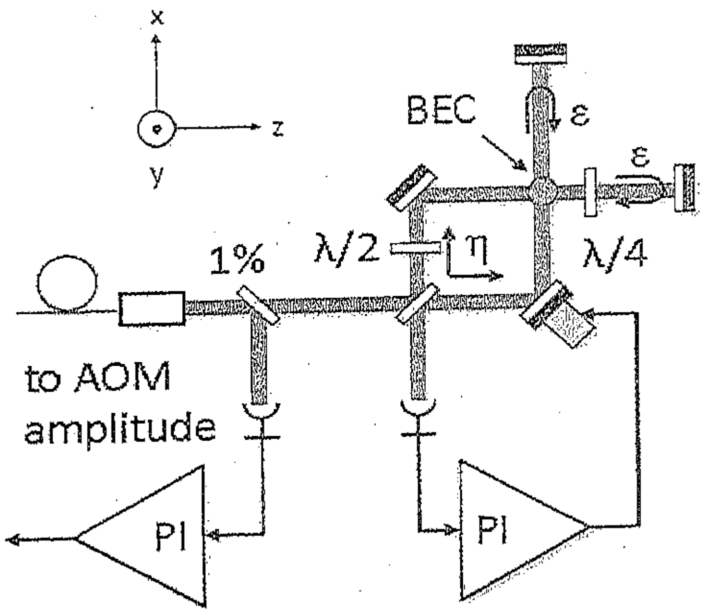

- monochromatic optical lattice with adjustable time-phase difference
- Michelson interferometer with vertical polarization, branches overlap perpendicularly, lattice forms in overlapping region
- Piezo-driven mirror to adjust relative phase difference θ in plane waves
- waveplates rotate polarization by α to compensate backreflection losses ε

$$-\frac{\bar{V}_0}{4}\, e^{-\frac{2z^2}{w_0^2}} \left|\eta\left[(\hat{z}\cos(\alpha)+\hat{y}\sin(\alpha))\, e^{ikx} + \epsilon\,\hat{z}\, e^{-ikx}\right] + e^{i\theta}\,\hat{z}\left(e^{iky}+\epsilon\, e^{-iky}\right)\right|^2,$$

For $\varepsilon=1$, $\alpha=0$:

$$-\frac{V_0}{2}\left(\cos 2k_l x + \eta^2 \cos 2k_l y + 4\eta\cos\theta\cos k_l x\cos k_l y\right)$$

$\theta = 0$ $\qquad$ $\theta = \pi/2$ $\qquad$ $\theta = \pi$

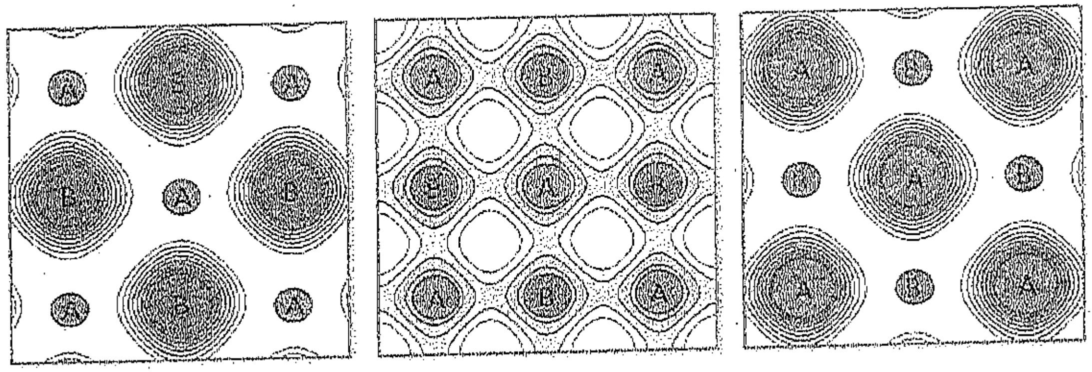

http://photon.physnet.uni-hamburg.de/fileadmin/user_upload/ILP/Hemmerich/miniMOT/Ischgl_2010_Wirth_6.pdf

P-bands [Wirth et al., Nature Physics 7, 147 (2010)]

Square lattice of two classes of tube-shaped sites

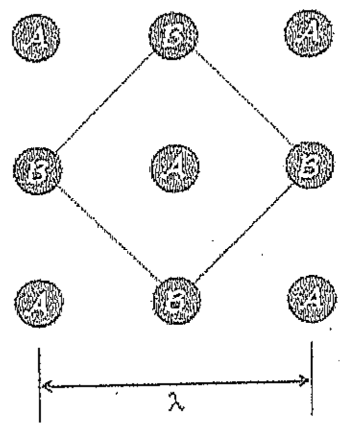

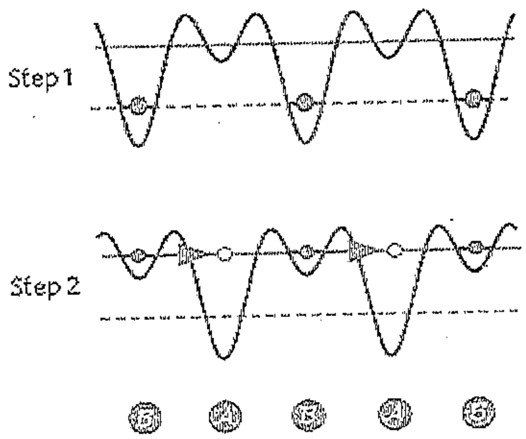

Transfer into p-band

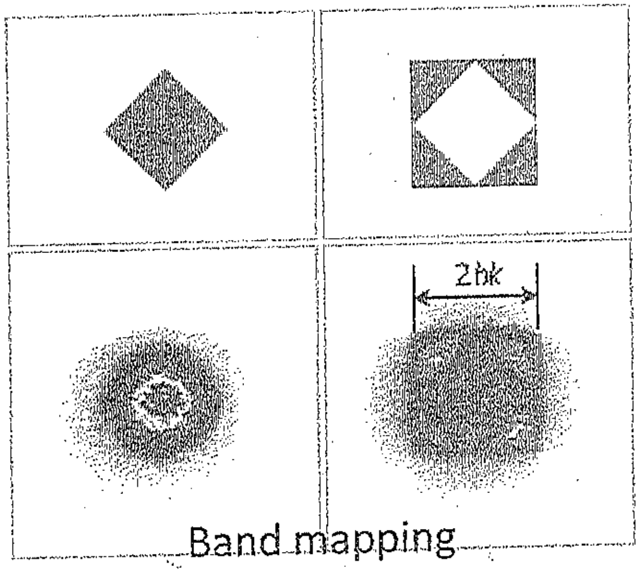

Band mapping

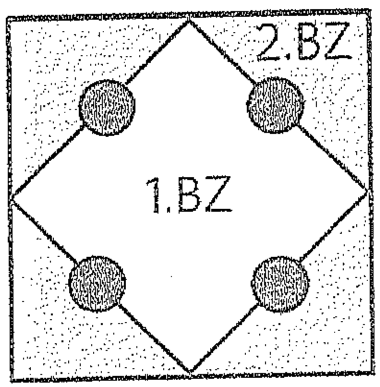

Degenerate points at the edges of the p-band

The degeneracy of the two points may be adjusted experimentally with the value of α

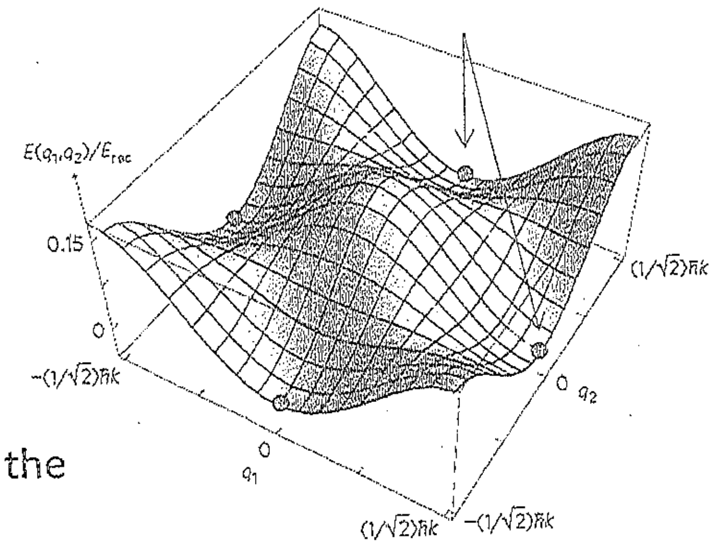

P-bands [Wirth et al., Nature Physics 7, 147 (2010)]

Asymmetric case

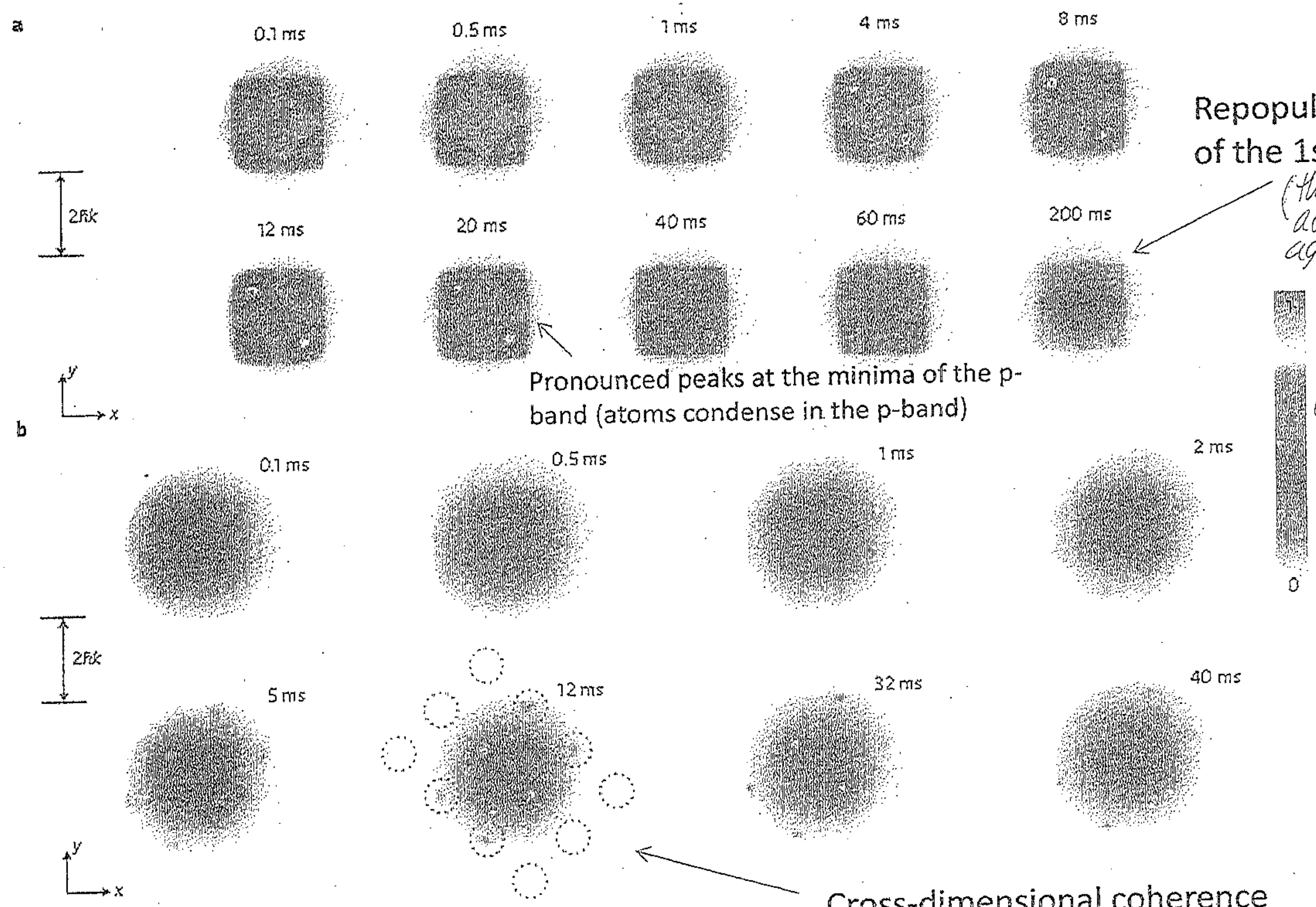

Repopulation of the 1st BZ

(the upper band is actually unstable against collisions)

(since only A sites are in our upper band this enhances lifetime to ~50ms, enough for P-band condensate)

Pronounced peaks at the minima of the p-band (atoms condense in the p-band)

Cross-dimensional coherence

P-bands [Wirth et al., Nature Physics 7, 147 (2010)]

Symmetric vs. asymmetric case

Repulsion favors Px+-iPy orbitals at A sites: Complex BEC !!

Symmetric

Phase transition controlled by α

Asymmetric

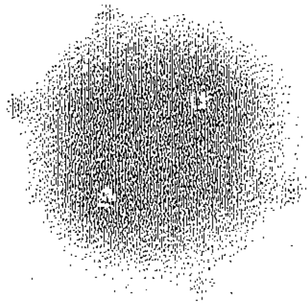

For sufficient asymmetry one recovers a real BEC (px+-py favoured: striped order with zero local angular momentum)